The Hubbard Model

Noah J. Song

April 2025

1 Introduction

Magnetic behavior occurs when the balance between spin-up and spin-down electrons breaks, either globally or locally. Transition metal systems often exhibit magnetism not captured the independent-electron approximation. In these cases, Coulomb repulsion complicates energy minimization, resulting in the spins in a solid to become aligned (ferromagnetism) or anti-aligned (antiferromagnetism).

John Hubbard introduced the Hubbard model in 1963 to capture electron motion and local interactions.[1]. Originally dedicated to studying electronic correlation effects in narrow bands, the model describes electrons moving across a lattice while experiencing an on-site Coulomb repulsion whenever two electrons with opposite spins occupy the same site. The model forms the foundation for modern methods such as DFT+U (Density Functional Theory + Hubbard U) and DFT+DMFT (Density Functional Theory + Dynamical Mean-Field Theory) to study condensed matter physics.

1.1 Motivation and Goals

This project on the Hubbard model follows the work of Claveau et al (2014)[2]. We will reproduce their energy band and energy of states results for $U = 0, t/U = 0.077, t/U = 0.2$.

To this end, this section concludes by introducing the theoretical background. The following section will give the results, and we will conclude with a discussion of potential future work.

1.2 Theoretical Backdrop

1.2.1 The Hamiltonian

Built on the language of second quantization, the core of the Hubbard model is the Hamiltonian:

$$\hat{H}_H = -\sum_{ij\sigma} t_{ij}\hat{c}^\dagger_{i\sigma}\hat{c}_{j\sigma} + U\sum_i \hat{n}_{i\uparrow}\hat{n}_{i\downarrow} \equiv H_t + H_U$$

where $\hat{n}_{i\sigma} \equiv \hat{c}^\dagger_{i\sigma}\hat{c}_{i\sigma}$ are the **occupation numbers** for spin σ, and $\hat{c}^\dagger_{i\sigma}, \hat{c}_{i\sigma}$ are the **creation and annihilation operators**, respectively. They act as instantiations and deconstructions of an electron at site i of spin σ.

The variable t_{ij} is called the **hopping amplitude**; thus H_t is a term that dictates the "travel" of electrons in our system. We will restrict the hopping to a particle's "nearest neighbors". Formally, we can write t_{ij} as

$$t_{ij,\sigma} = \int d^3\vec{r}\,\varphi^*_{\vec{R}_i,\sigma}(\vec{r})\left(-\frac{\hbar^2\nabla^2}{2m} + V(\vec{r})\right)\varphi_{\vec{R}_j,\sigma}(\vec{r}).$$

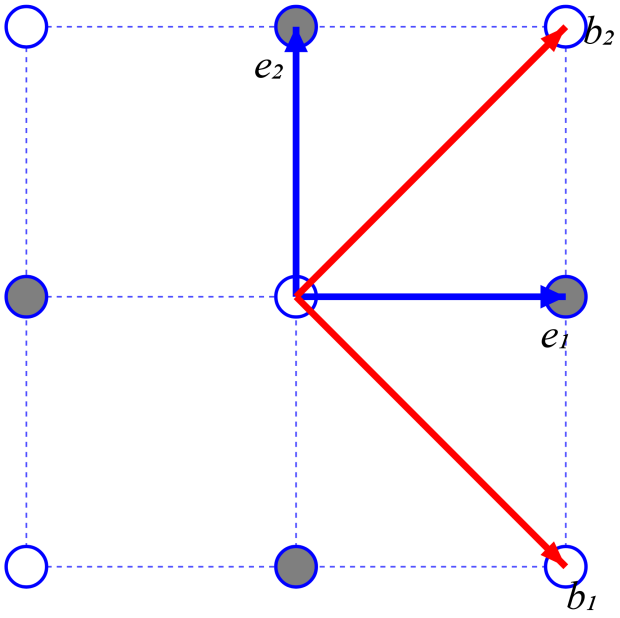

Figure 1: Our basis should be such that it contains two sites per unit cell.

The variable U is given by a familiar expression,

$$U \equiv \frac{e^2}{4\pi\varepsilon_0} \int \mathrm{d}^3\vec{r}\,\mathrm{d}^3\vec{r}' \, |\varphi_{\vec{R}_i,\sigma}(\vec{r})|^2 \frac{1}{|\vec{r}-\vec{r}'|} |\varphi_{\vec{R}_i,\bar{\sigma}}(\vec{r}')|^2,$$

where $\varphi_{\vec{R}_i,\sigma}(\vec{r})$ is centered at exactly $\vec{R}_i$. Another restriction of the Hubbard model is that this Coulomb repulsion only applies where electrons inhabit the same site, as seen from the Hamiltonian.

1.2.2 The Fourier Transform

We simplify our study of the Hamiltonian by moving to the **reciprocal space**, the Fourier transform of real space. Since we want to study antiferromagnetic states, it is thus necessary to study neighboring sites. We will call this basis set $\mathscr{B} = \{b_1, b_2\}$. 1.

We omit the Hamiltonian transformation for brevity. The derivation can be found in Claveau [2], and ultimately leads to a Hamiltonian

$$\hat{H}_{\tilde{H},\sigma,\vec{k}} = \begin{bmatrix} U\langle n_{1\bar{\sigma}}\rangle & t\gamma_{\vec{k}} \\ t\gamma^*_{\vec{k}} & U\langle n_{2\bar{\sigma}}\rangle \end{bmatrix},$$

where $\gamma_{\vec{k}} = -\left\{1 + e^{-i\vec{k}\cdot(\vec{b}_1+\vec{b}_2)} + e^{-i\vec{k}\cdot\vec{b}_1} + e^{-i\vec{k}\cdot\vec{b}_2}\right\}$ and $\bar{\sigma}$ denotes the spin opposite to σ.

So our process will entail

- Picking n_e and a range of $\vec{k}$ values
- Calculating $\gamma_{\vec{k}}$ for each $\vec{k}$
- Diagonalizing the Hamiltonian to obtain the wavefunction for $\vec{k}$, spin σ, and n_e.

The eigenvalues of H_H have an analytical form, but we simply use Julia's LinearAlgebra "eigen" solver.

We note that for cases $U \neq 0$, we will need to perform this diagonalization twice: once for the spin up case, and once for spin down. Each operation will result in two wavefunctions, so that in the Brillouin zone, we will see four different bands.

We compute the wavefunctions and the system's **density of states**:

$$\rho(\varepsilon) = \frac{1}{N} \sum_{\vec{k},j,\sigma} \delta[\varepsilon - \varepsilon_{j\sigma}(\vec{k})]$$

where N is the number of sites in the unit cell. Conceptually, this is the number of electronic states at a given energy. This metric allows us to study the critical points in the wavefunctions, which might give rise to Van-Hove singularities or other peculiar behavior.

To compute the Dirac-delta function, we make use of Gaussian functions whose smearing width is 0.05, replacing a discrete landscape with a sum of Gaussians, which are continuous.

2 Results

2.1 The Tight-Binding Solution

We begin for the simpler case where $U = 0$. Physically, this means that electrons have no "cost" for residing on the same site, and that the hopping dynamics are the sole parameter for the band structure.

We note that for computational purposes, we nondimensionalize to treat our energies in terms of t.

Our results are in in figures 2 and 9. They are exact, which is expected - our calculations are deterministic in the sense that there is no randomness in the calculation of the band. Changing the basis set does not alter the system's physics. The double cell, being double the size of the single cell, results in a Brillouin zone that is exactly half of its original size. The mirrored result is simply the same band folded into smaller the Brillouin zone.

2.2 Ferromagnetic and Antiferromagnetic States

We expect to get more sophisticated results as we vary t/U, as opposed to the prior section. As for technical details, we used a k-point mesh density of 500×500, the same as in the paper. All the results in this section used constants of $n_e = 1.6$.

When t/U is small, giving strong interactions within sites, electrons tend to localize and align their spins to minimize double occupancy, meaning we see a more significant magnetic order. Our magnetic order depends on t/U and the density of electrons. For $n_e = 1.6$ and $t/U = 0.077$, our results show a ferromagnetic phase.

Figure 8 shows the shifted spin-up and spin-down bands, producing unequal spin populations. On the other hand, for $t/U = 0.2$, the antiferromagnetic regime exhibits an opening of a Slater gap at the new zone boundary. Our mean-field Hamiltonian H_H causes this phase.

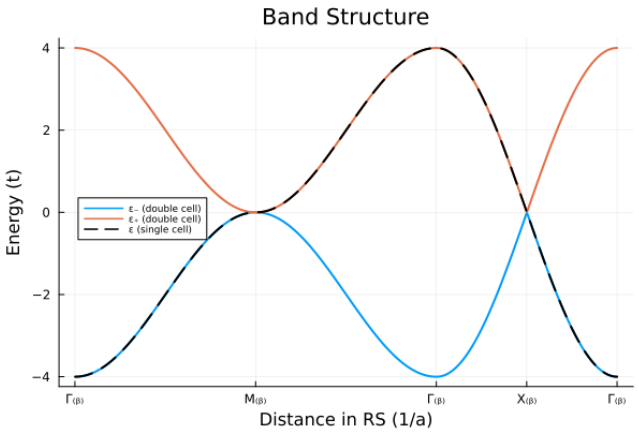

Figure 2: A re-derived band structure using Julia

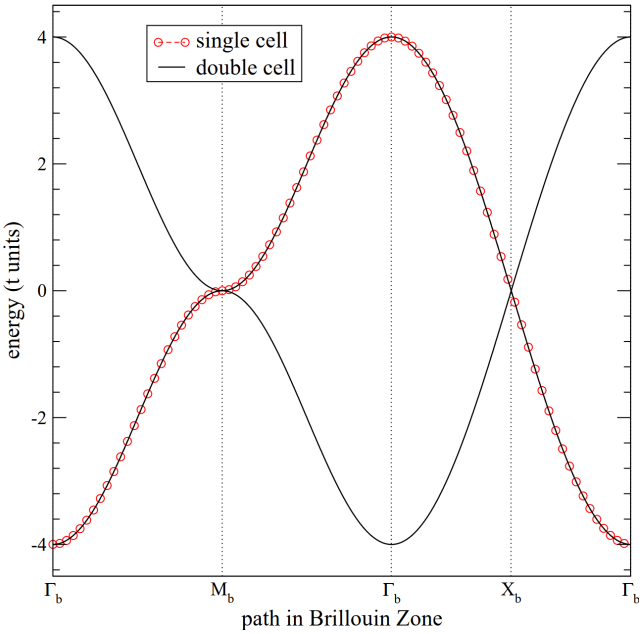

Figure 3: The tight binding solution given in the paper

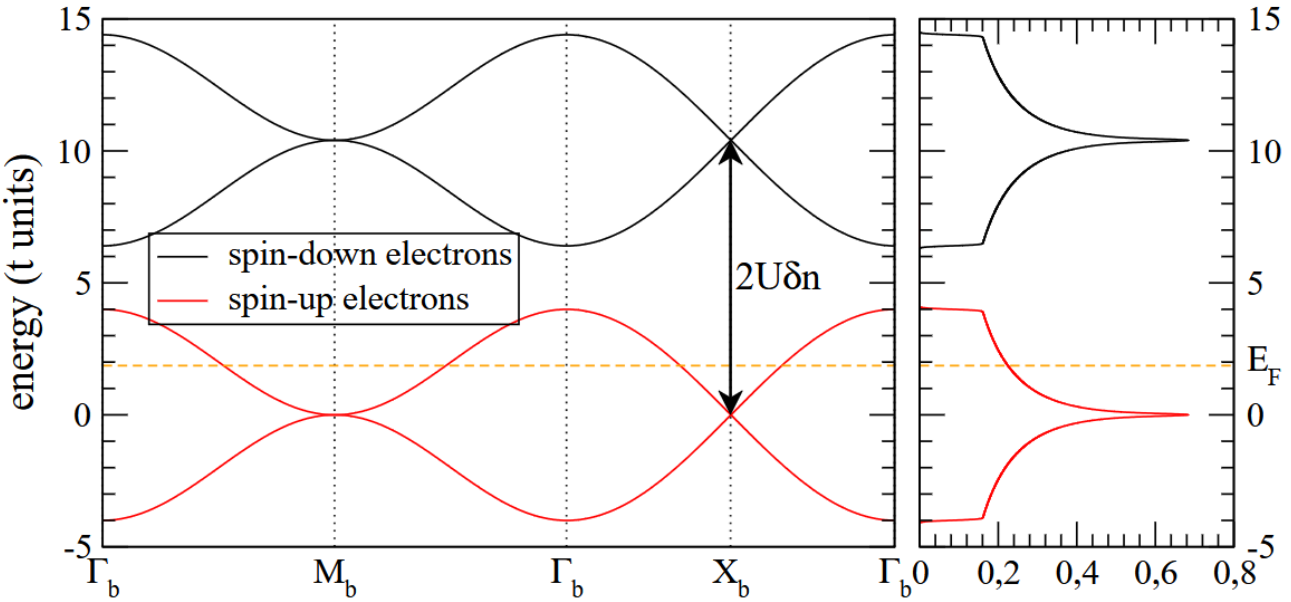

Figure 4: Ferromagnetic band structure and DOS given in Claveau

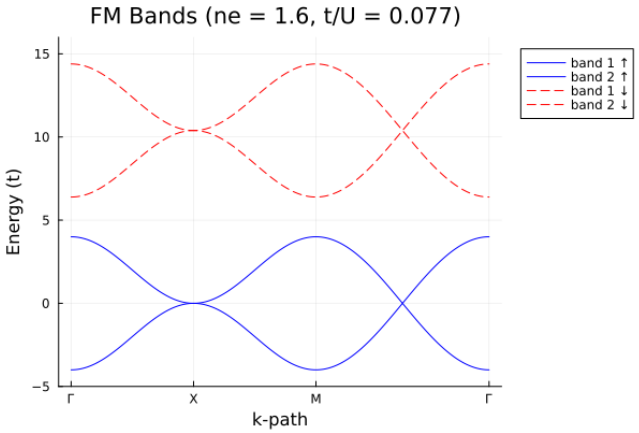

Figure 5: Re-derived FM band structure with $n_{1\uparrow} = n_{2\uparrow} = 0.8$, $n_{1\downarrow} = n_{2\downarrow} = 0.0$

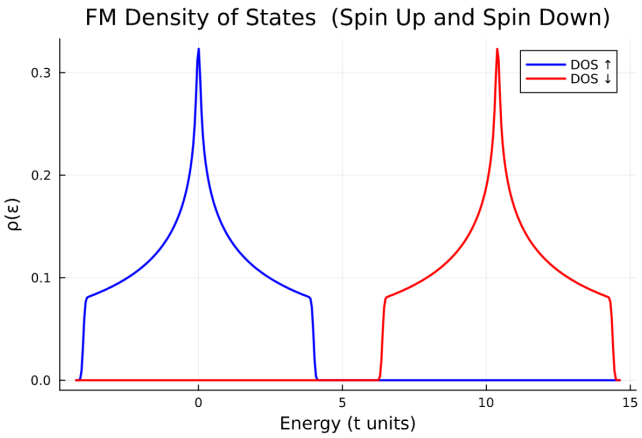

Figure 6: The FM density of states

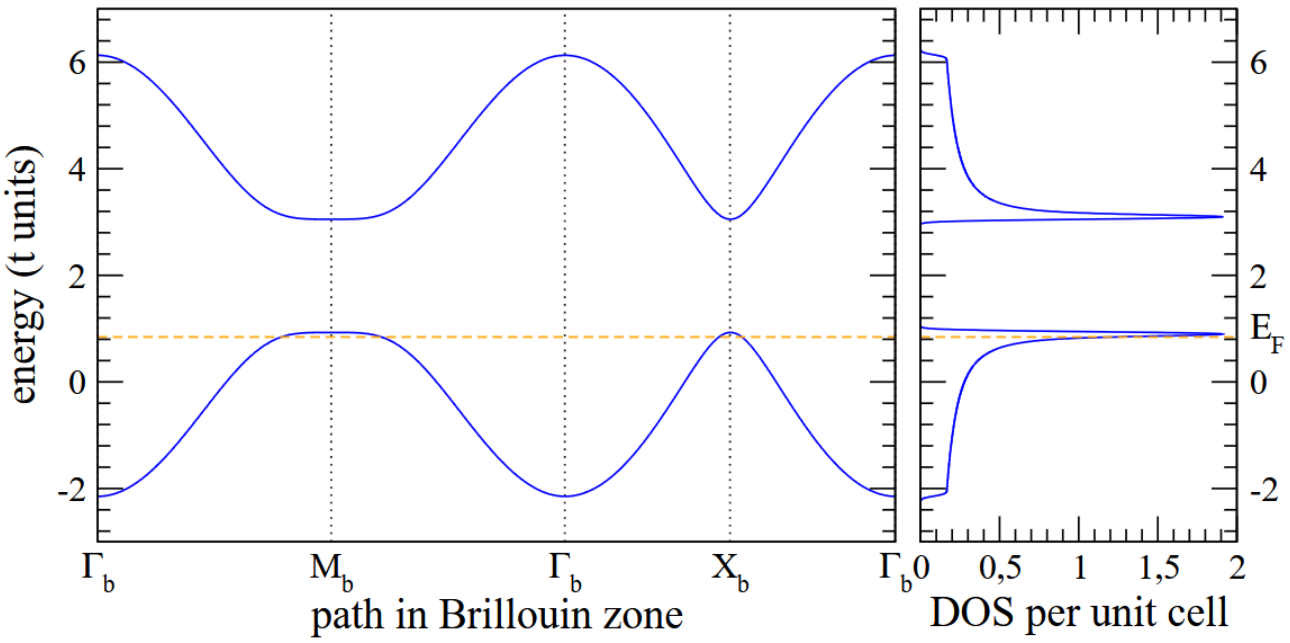

Figure 7: Antiferromagnetic band Structure and DOS calculated by Claveau

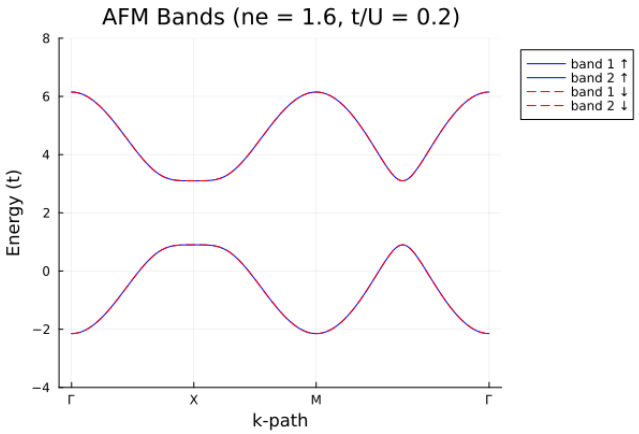

Figure 8: Re-derived AFM band structure with $n_{1\uparrow} = n_{2\uparrow} = 0.62 n_{1\downarrow} = n_{2\downarrow} = 0.18$

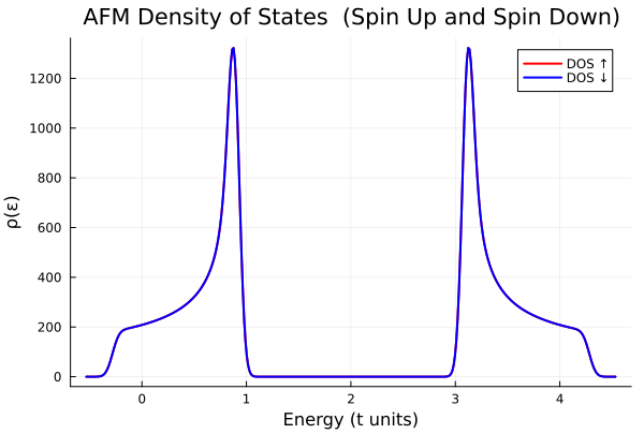

Figure 9: The AFM density of states

Our FM and AFM band structures match those of Claveau et al. (2014). One difference comes from the notation of the points in the Brillouin Zone, but this is a result of simply using different basis sets in our $k-$path.

3 Conclusions

We successfully reconstructed key aspects of the Hubbard model's behavior on a two-dimensional square lattice, focusing particularly on the differences in band structure in ferromagnetic and antiferromagnetic states. We were ultimately able to recover the correct band structures and investigate the corresponding density of states for different interaction strengths t/U.

As a test case, we used the limit of vanishing Coulomb repulsion ($U = 0$) to confirm the tight-binding solution and observed the expected band folding arising from the halving of the Brillouin zone. When $U \neq 0$, we observed characteristic features of ferromagnetic and antiferromagnetic ordering, including band splitting and the opening of gaps. Most importantly, our results matched nearly exactly with those of Claveau et al. (2014).

Regrading future work, one immediate next step pertains to plotting the full phase diagram using mean field techniques, as described in Claveau. Afterwards, the paper suggests implementing next-nearest-neighbor hopping or multi-orbital effects, and as noted in the Introduction, can be extended into modern condensed matter techniques.

References

[1] J. Hubbard. Electron correlations in narrow energy bands. *The Royal Society*, 1963.

[2] S. Di Matteo Y. Claveau, B. Arnaud. Mean-field solution of the hubbard model: the magnetic phase diagram. 2014.